Hot Wire Measurements Downstream of a Propfan

T. G. Tillman* and J. C. Simonich†
United Technologies Research Center, East Hartford, Connecticut 06108

The problem addressed in this article is the analysis of propfan near-field aerodynamics. The wake structure was examined for a counter-rotation propfan model operating in the single-rotation mode. The goal of the present effort was to obtain a set of experimental near-field propfan aerodynamic data that defined the rotor synchronized downstream flowfield for a simulated cruise condition. Specifically, three components of blade-synchronized periodic velocity were obtained, with particular attention given to the blade tip region. The present approach employed a high-frequency response hot wire anemometer system to measure the three components of velocity at various radial locations during the course of a blade passage. In addition, blade surface flow visualization was performed to help characterize leading edge vortex features. As a result of this study, a set of data defining the propfan wake structure was obtained, including definition of the vortex region. Tip region wake roll-up features were qualitatively identified, and the existence of a vortex core axial velocity defect was documented.

Nomenclature

B = number of blades on rotor
h = hot wire binormal velocity calibration constant
J = propeller advance ratio, = $(\pi M_0/M_T)$
M_T = blade tip Mach number
M_0 = wind-tunnel freestream Mach number
P = static pressure
R = propeller radius
r = radial distance
T = period of blade rotation; temperature
t = time
U = velocity
U_{eff} = hot wire effective cooling velocity
u = flowfield axial velocity (positive downstream)
v = flowfield tangential velocity (positive opposite blade rotation)
w = flowfield radial velocity (positive outward)
x = axial coordinate
y = tangential coordinate
z = radial coordinate
α = angle of attack
α_a = propeller advance angle, = $(\tan^{-1}[M_0/M_T])$
β = propeller blade pitch angle
Γ = circulation
ϕ = propeller swirl angle, = (90 deg − α_a)

Subscripts
0 = wind-tunnel freestream condition

Introduction

THE problem addressed in this article is the analysis of the near-field aerodynamics of a profan flowfield. The wake structure was examined for a simulated cruise operating condition, where a reduced tip Mach number was set at the cruise design advance ratio, blade pitch angle, and nondimensional blade loading. Thus, the operating condition simulated all of the cruise aerodynamics with the exception of compressibility and Reynolds number effects. Understanding the details of the aerodynamics in the vicinity of a propfan is important for several reasons. Since propfans are designed for operation in counter-rotation, understanding how the wakes and vortex regions develop from an upstream blade row and how they impact the downstream blades is important from the standpoint of propfan noise and structural response. Since propfan aerodynamics have recently been shown to be very complicated, with features such as leading-edge vortices present, understanding the details of the near-field propfan flowfield is critical to blade design and performance prediction efforts.

Until recently, very little experimental work has been published on propfan flowfields. Hanson and Patrick[1] performed hot wire measurements and analytical calculations downstream of a single rotation advanced turbopropeller (SR-3) operating at a supersonic tip speed in a low speed, open jet wind tunnel. That paper explains much of the wake physics for the given propeller geometry and an operating condition that matches the tip Mach number, but lacks other features of a true cruise simulation (i.e., advance ratio and blade loading). Podboy and Krupar[2] measured the wakes both between and downstream of the rotors of an unducted fan counter-rotation model operating at a cruise-like condition (J = 2.8). Their experiment employed the use of a laser Doppler velocimetry (LDV) system that could be synchronized to either rotor, but not to both simultaneously. Therefore, the data acquisition process time averaged the unsteady influence of the nonsynchronized rotor on the periodic velocity data. This undesirable effect may be particularly important when measurements are performed between the two rotors.

Hanson[3] presents results that identify the presence of a leading-edge vortex on counter-rotation propfan (CRP) blades. This finding was the result of a 1986 experiment that employed a surface flow visualization technique.[4] This discovery demonstrated the need for further research into understanding the details of the propfan downstream flowfield, particularly in the blade tip near-field region. In light of this fact, the overall goal of the present effort was to obtain a set of aerodynamic data defining the three-dimensional downstream flowfield of a five-bladed, model scale propfan (CRP-X1) operating at a simulated cruise condition in the single-rotation mode. Specifically, blade-synchronized, three-dimensional periodic velocity measurements over both the passage of a single blade as well as the passage of all five blades were desired. Particular attention was paid to the downstream blade tip region. The single-rotation mode was chosen for study since it eliminated the need to account for the presence (i.e., synchronization) of the second rotor in the data acquisition and data reduction process. Although this experiment did lack the influence of the second rotor on the flowfield, it allowed for the accurate and thorough documentation of the wake

Received June 29, 1990; revision received Sept. 10, 1990; accepted for publication Sept. 24, 1990.

*Research Engineer. Member AIAA.
†Senior Research Engineer. Member AIAA.

structure associated with a single propfan blade row. This is viewed as a good starting point for detailed research of propfan flowfields. The present approach employed a high-frequency response hot wire anemometer system to measure three orthogonal components of blade-synchronized periodic velocity. Blade surface flow visualization was performed to help characterize the leading-edge vortex features.

As a result of this study, a set of aerodynamic data defining the downstream flowfield of a propfan was obtained. This includes definition of the downstream vortex region. Qualitative wake roll-up features were identified, which may be important in understanding propfan noise and performance. In addition, a vortex core axial velocity defect was discovered, which represents a possible CRP interaction noise source.

Description of Experiment

Experimental Arrangement

The present experimental study was performed in the United Technologies Research Center Open Jet Acoustic Wind Tunnel. A paper describing the design of the tunnel is given by Paterson et al.[5] The tunnel is of the open circuit, atmospheric type and is powered by a single-stage, 1500-hp centrifugal fan. A 46-in.-diam test section was used in the present experiment. Figure 1 shows a schematic diagram of the wind tunnel.

A five-bladed, 24.5-in.-diam, single-rotor propfan model was employed in the present experiment. This particular model required the removal of the front rotor assembly when single-rotation operation was desired. Thus, the rear rotor assembly of the CRP-X1 was used and the front rotor was removed and replaced with a nonrotating bare hub. The front and rear rotors were aerodynamically similar and rear rotor wakes were felt to be representative of front rotor wakes (barring potential field and dual-rotor coupling effects). The model was powered by an air turbine drive rig, which was capable of turning the rotor up to 12,000 rpm. Propeller rotational speed could be held constant to within ±25 rpm.

Experimental Program Definition

The primary objective of the present experimental study was to obtain three components of periodic velocity at discrete points within the flowfield downstream of the propfan. Three separate measurements at each location, employing three different hot wire probe orientations, were required in order to obtain the three-dimensional velocity field. The velocities measured were steady (i.e., mean velocities) in the sense that the hot wire voltages were synchronously averaged over thousands of blade passages. They were unsteady in the sense that data acquisition was synchronized with the blade passage, so that points were obtained at discrete intervals of rotor position as the blade moved past the probe. This allowed for blade wake features to be distinguished. In addition to measuring the velocity field, blade surface flow visualization was also performed to study the propfan leading-edge vortex/tip vortex features.

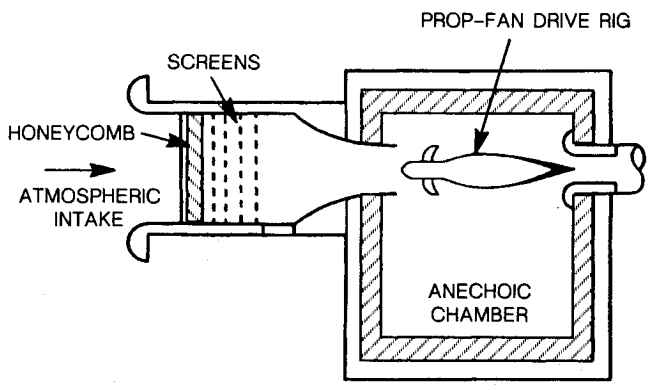

Fig. 1 UTRC open jet acoustic wind tunnel.

Hot wire measurements were made at several radial locations downstream of the propeller. These measurements were performed along a line making a 25-deg angle with the blade plane of rotation such that the line passed 5-in. downstream of the blade tip at $r/R = 1.00$. This survey line was chosen because it approximates the quarter chord location of the downstream rotor in a counter-rotation installation. One of the motivations for performing this experiment was to gain an understanding of the CRP interaction noise and aerodynamics associated with the impingement of upstream blade wakes on the downstream rotor. Acquiring the data along a simulated downstream rotor quarter chord line allows for analytical noise and performance predictions to be performed, which use the measured wakes as one input to the calculation. The radial stations for recording data points covered a range of r/R from 0.4 to 1.1, with a dense spacing of stations in the tip region so that good resolution of the tip vortex/leading-edge vortex could be achieved.

Measurements were performed for a simulated cruise operating condition. The tunnel freestream Mach number was 0.25, with the blade tip Mach number 0.276. This combination provided an advance ratio of 2.85 at a nominal rpm of 2900. The blade surface nondimensional pressure distribution and model power coefficient were both simulated relative to the actual cruise case. Thus, the present simulation lacked only compressibility effects and some Reynolds number effects, and Reynolds number effects were expected to be small. It should be noted that advance ratio was held constant for the various runs for each case by slightly adjusting the rpm to account for varying ambient conditions.

Instrumentation

A 10-channel, Thermo Systems, Inc., (TSI) IFA-100 constant temperature hot wire anemometer system[6] was used to perform the measurements in the present experiment. A 1:1 bridge was used in order to achieve a high system frequency response. The bridge was operated with fixed control resistors, with a duplicate probe cable placed between the control resistor and the bridge in order to balance the bridge impedance. Cylindrical 0.002-in.-diam hot film sensors (TSI models 1211 and 1213) were used with the anemometer primarily due to their rugged construction. It was found that sufficiently high frequency response could be achieved with these sensors in the present application.

Prior to the experiment, the hot wire anemometer system frequency response was checked electronically by employing standard square wave testing techniques.[7] The testing was done at an airspeed of 300 ft/s, which was approximately the wind-tunnel freestream airspeed during the experiment. Test results yielded cutoff frequencies in the 300–500 kHz range using the cylindrical hot film sensors and 40-ft probe and control resistor cables.

It should be noted that in most hot wire applications the measurement of high-frequency velocity fluctuations (those >100 kHz) is difficult. This is because a typical turbulence signal at the high end of the frequency spectrum is very weak and may be lost in the internal anemometer electronic noise. In the present experiment, high-frequency response was desired in order to resolve spatially thin aerodynamic features that were locked to the propeller and rotating past the hot wire probe at high speed. Although the features themselves were spatially small (i.e., thin viscous wakes), the signals associated with them were large compared with background noise levels and their dimensions were large relative to high-frequency turbulence length scales. Thus, the high-frequency fluctuations encountered in the present study were of sufficient amplitude that the internal anemometer noise was not a problem.

The details of the hot wire measurement technique used in the present experiment are described by Tillman et al.[8] This technique is based on that of Hanson and Patrick,[1] where two hot wire probe geometries were used (with one employed in two separate orientations) to provide the three independent

measurements needed to document the three-dimensional velocity field.

An oil/fluorescent tracer method was used in the present study to examine blade surface flow features. This method involves the use of a mixture of tracer pigment suspended in a suitable weight of oil, which is painted on the model and allowed to flow under the action of forces exerted on it by the airstream. The tracer pigment leaves behind streaks that indicate surface flow direction. Since the tracer pigment is fluorescent, the streak pattern is highly visible and easy to photograph under ultraviolet light. In the case of rotating models, there is a centrifugal force that also acts on the oil, complicating the interpretation of surface flow features. Useful surface flow information may still be obtained in the presence of this force, as described by Tillman et al.[8] A thorough description of this flow visualization technique as applied to propfan blades is offered in the literature.[4,8]

Data Acquisition

The data acquisition process for sampling the hot wire output voltages is shown schematically in Fig. 2. The raw bridge output signal contains random as well as phase related information. In order to remove the random component, the bridge output was digitally averaged approximately 4000 times using an ensemble averaging technique. To generate the data sample increment, a rotor once per rev signal (pip) was fed into a Signal Dynamics Model 134A Tracking Ratio Tuner. This device is capable of tracking a variable frequency input signal and providing an output signal that is a multiple of the input frequency. The multiplied output from this device was used as the sample increment. For the present experiment, the multipliers that were used were 1600 and 400, which digitized a little more than one blade passage or all five blade passages, respectively. A conditioned version of the pip signal was used to initiate the data acquisition process. The majority of the experimental data was acquired over a single blade passage. A few sets of the complete five-bladed data were taken in order to check aerodynamic blade-to-blade variations of the model. The nominal digitization rate that resulted from this process was 77 KHz for data acquired over a single-blade passage and 19 KHz for data acquired over the passage of all five blades.

The bridge output signal was digitally enhanced using a Honeywell SAI-48 Correlator and Digital Signal Averager. This instrument uses the frequency multiplied signal from the tracking ratio tuner output to sample the hot wire signal at discrete increments of rotor position. In this way, during averaging, slight variations in rotor rpm do not smooth out any sharp features of the data since digitization is linked to the direct position of the rotor and not the relative position based on a time delay since the pip signal. The SAI-48 is a high-speed device that uses a variable resolution analog to digital converter (3 and 9 bits) and a dithering technique to achieve 12 bits of accuracy. The digital data were transferred to a VAX 11/750 computer for storage and processing.

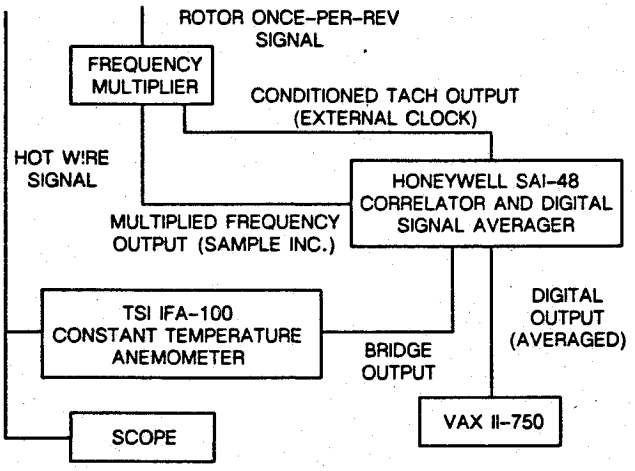

Fig. 2 Hot wire synchronous sampling data acquisition.

Results and Discussion

Hot Wire Data

Velocity Time History

The results of the hot wire measurements for 10 of the 15 radial stations acquired are presented in Fig. 3. This figure shows plots of axial, tangential, and radial velocity components, normalized by the wind-tunnel freestream velocity, as a function of the parameter Bt/T. The sign convention is such that positive axial velocity is in the downstream direction, positive tangential velocity is opposite to the direction of blade rotation, and positive radial velocity is outward from the hub. Bt/T is a nondimensional time, with B equal to the number of blades on the rotor (five), t the time, and T the period of rotation for the entire rotor. Thus, $Bt/T = 1$ corresponds to one fifth of the rotor revolution, or one blade passage, $Bt/T = 2$ corresponds to two fifths of the rotor revolution, or two blades, etc. The data shown in Fig. 3 were acquired over 1.25 blade passages. Note that the vertical scales in this figure have been adjusted at each radial station to provide maximum visual resolution of the wake structure. In some cases, this results in the misconception of increased data scatter. When studying the data in Fig. 3, these varying scales should be examined carefully.

As seen in Fig. 3, axial velocity viscous wakes are present out to $r/R = 0.94$. These velocity defects are approximately 5% of the peak axial velocity at each radial location up to $r/R = 0.8$. It should be noted that the axial velocity viscous and potential wake effects are opposing, and separating the two is difficult. What is referred to in the present study as an axial velocity viscous wake is actually the net result of both effects.

As pointed out by Hanson and Patrick,[1] the character of the radial velocity is related to the circulation distribution on the blade. The strength of the trailing vorticity is proportional to $d\Gamma/dR$, and this vorticity most clearly shows up as a jump in the radial velocity component w. The sign of the jump depends on the sign of $d\Gamma/dR$. The theoretical circulation distribution for the present propfan blade starts at a low value in the inboard region, rises to a maximum in the vicinity of $r/R = 0.7$, and falls sharply to zero at the tip. The radial velocity data of Fig. 3 agree quite well with this expected behavior. At $r/R = 0.5$ and 0.6, progressively smaller positive jumps in radial velocity are observed as the blade passes, corresponding to a positive but decreasing $d\Gamma/dR$. At $r/R = 0.7$, there is virtually no radial velocity jump. Outboard of this location the jump is negative, corresponding to negative $d\Gamma/dR$. The magnitude of the jump increases as the blade tip is approached and values of $d\Gamma/dR$ become more negative. The behavior of this velocity component does, in fact, seem to provide a useful means to experimentally verify theoretical blade loading distributions.[1]

Effects of the tip vortex/leading-edge vortex begin to be seen in the vicinity of $r/R = 0.90$. In this region, a hump begins to appear in the axial velocity trace just after the viscous wake. In addition, the tangential and radial velocity components start to exhibit features of skewing, or roll-up, of the trailing vortex sheet. This effect will be described later. Continuing outboard, the hump in axial velocity increases until it reaches a maximum height at $r/R = 0.96$. The presence of this axial velocity peak is due, in part, to the manner in which the blade tip vortex/leading-edge vortex convects downstream after leaving the blade. Neglecting rotor induction and mean wake flow effects, the vortex will follow a helical path downstream, with a trajectory that will approximate the propeller swirl angle $\phi = 90 \text{ deg} - \alpha_a$ relative to the x axis. This

results in the vortex swirl velocity (i.e., tangential) having a component that adds positively to the axial velocity on the inboard side of the vortex. This effect is partially responsible for the increase in axial velocity observed up to $r/R = 0.96$; acceleration due to local blade loading may also account for some of the increase. Figure 4 shows a diagram of the flow angles and velocities relative to the propeller blade in the tip region.

Looking back to Fig. 3, one notices a drastic change in the character of the axial velocity at $r/R = 1.00$. Here, there is a large velocity defect (approximately 15% of the peak velocity) associated with the outboard portion of the vortex. This characteristic persists outboard, as seen at $r/R = 1.02$. Here it has spread out slightly and diminished in magnitude. At $r/R = 1.10$ (not shown), the defect has broadened further and decreased to approximately 2% of the peak axial velocity at this station. One might presume that the outboard velocity defect is the result of the mirror image of the effect described earlier; that is, that the swirl on the outboard side of the vortex has a component that adds negatively to the axial velocity. Although this is true, it will be shown in the next section that this effect does not account for all of the velocity defect present on this side of the vortex. Hence, one is led to the conclusion that the propfan blade tip vortex/leading-edge vortex structure possesses an axial velocity defect in the outboard region.

As briefly mentioned previously, the tangential and radial components of velocity also possess unique features attributed to the presence of the vortex structure. At $r/R = 0.9$, the tangential velocity wake has become large. Note in this case that the viscous and potential wakes are additive (both in the direction of rotation), as opposed to the case of the axial velocity. Moving outboard from this point, the tangential velocity wake begins to spread out and show some complicated behavior in the form of perturbations to the wake profile. These features are also apparent in the radial velocity profile, which does not possess the discontinuous jump from radially outward to radially inward flow characteristic of a flat, unskewed vortex sheet. At $r/R = 0.96$, which is very close to the center of the vortex structure, both of these velocity components exhibit their sharpest features. At $r/R = 1.00$, the tangential velocity shows evidence that the outboard portion of the vortex has been reached. A positive pulse of velocity is now imparted as the blade passes, indicating vortex swirl in this direction. Continuing outboard from this point, the tangential and radial velocity profiles spread out with their features becoming less pronounced in magnitude, much like the axial velocity.

The data described up to this point were obtained over the passage of a single blade, with some overlap into the approach of the next rotor blade. In order to insure that the aerodynamics associated with this particular blade were representative of all of the blades of the rotor, measurements were performed to document the five-bladed flowfield. This was done by adjusting the frequency multiplied sample increment, as described earlier, so that the total sampling time (number of data points times the sample increment) was equal to the rotor period. It was found that the blade-to-blade variations of the wake velocity components were quite small; good agreement was obtained between the single-bladed measured flowfield and the five-bladed flowfield.

An analysis was carried out to study the effect of uncertainties in the data reduction inputs on the final reduced velocities. The details of the analysis, and the results, are de-

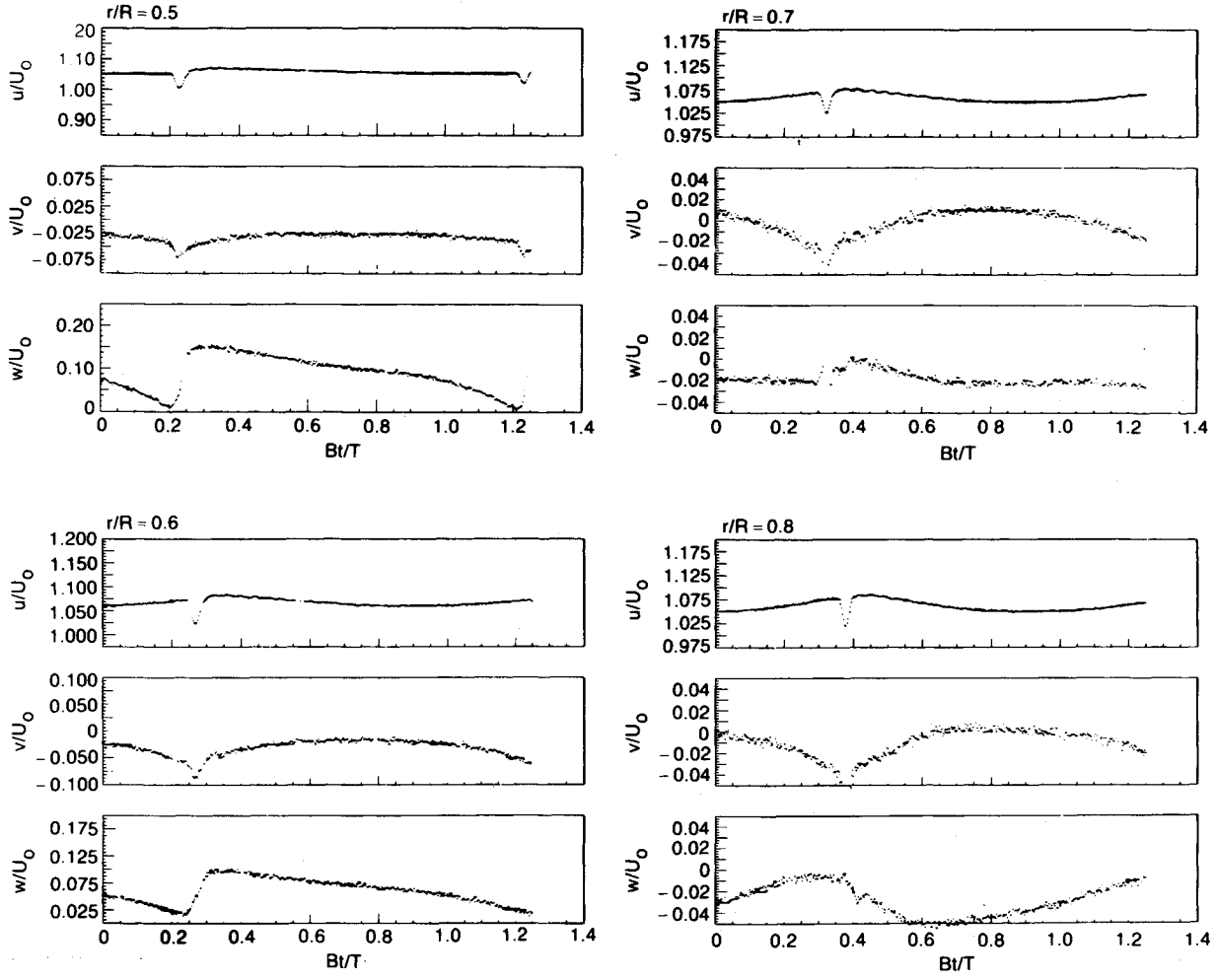

Fig. 3 Hot wire velocity data.

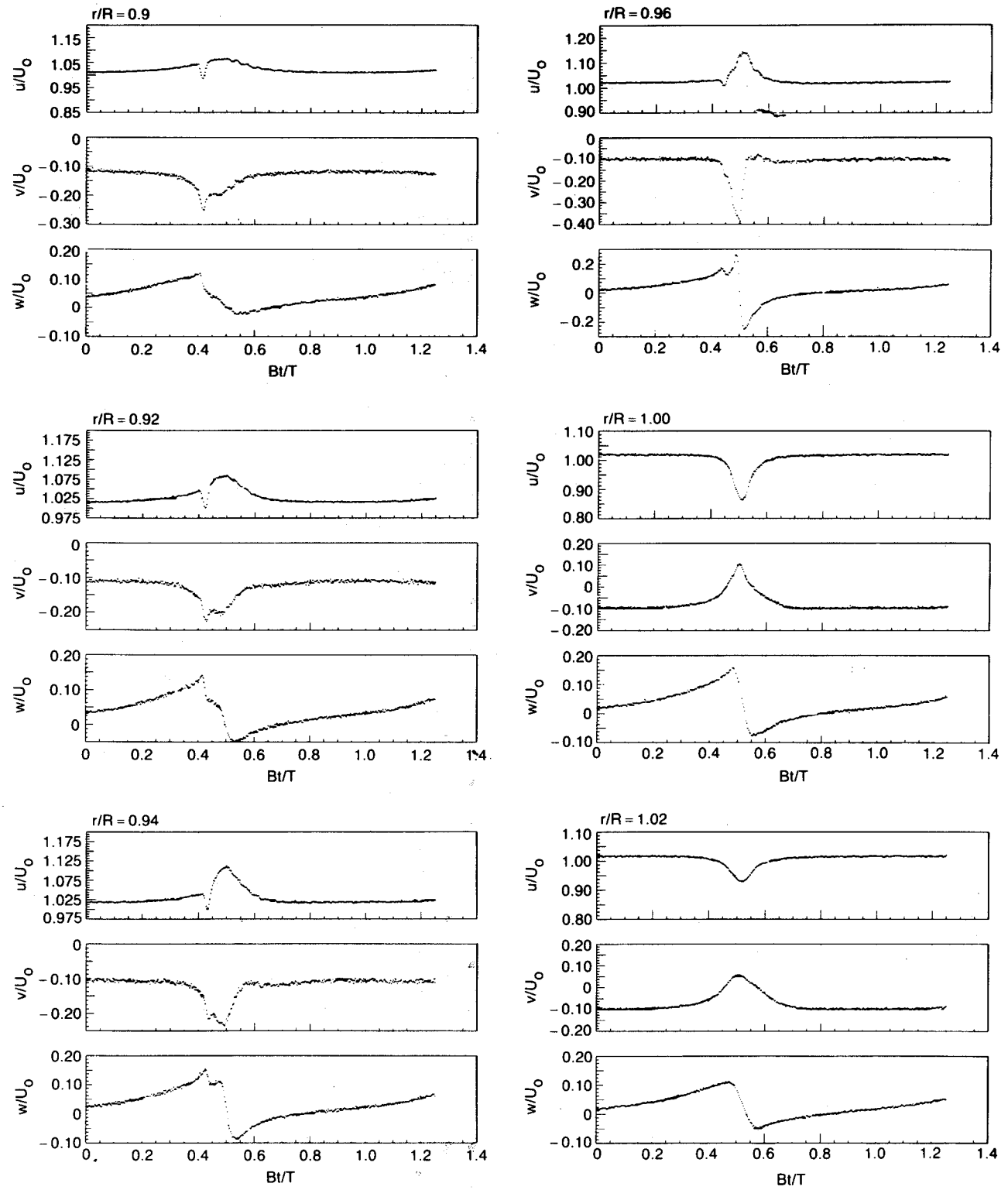

Fig. 3 (Continued) Hot wire velocity data.

scribed by Tillman et al.[8] It was found that the uncertainty levels in the data were acceptable, with a first-order uncertainty in the resultant total velocity vector magnitude (i.e., the vector combination of u, v, and w) of approximately $\pm 6\%$. In addition, it should be noted[8] that the data scatter that is present in Fig. 3 falls well within the estimated uncertainty band for each velocity component separately.

Three-Dimensional Flowfield

In order to gain a better understanding of the propfan flowfield, particularly in the blade tip region, the data for each of the radial stations ($r/R = 0.4$–1.1) were transformed from a time history to a position in space relative to the rotor. All of the 15 radial stations were then used to generate a complete map of the rotor flowfield in three-dimensional space. This technique for visualizing three-dimensional data is described by Edwards.[9] Figure 5 shows one form of presenting the data, which is a vector plot of the velocity in the propeller plane of rotation. This figure essentially represents a view from downstream looking upstream in the axial direction. The vortex region is clearly identified. Note that, for clarity, to prevent vectors from overlapping, only every tenth data point

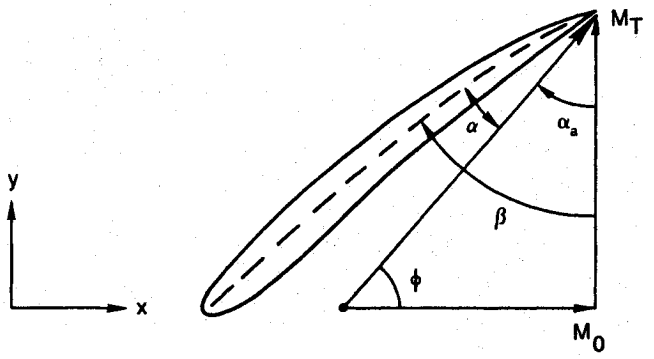

Fig. 4 Propeller tip region velocity diagram (relative frame).

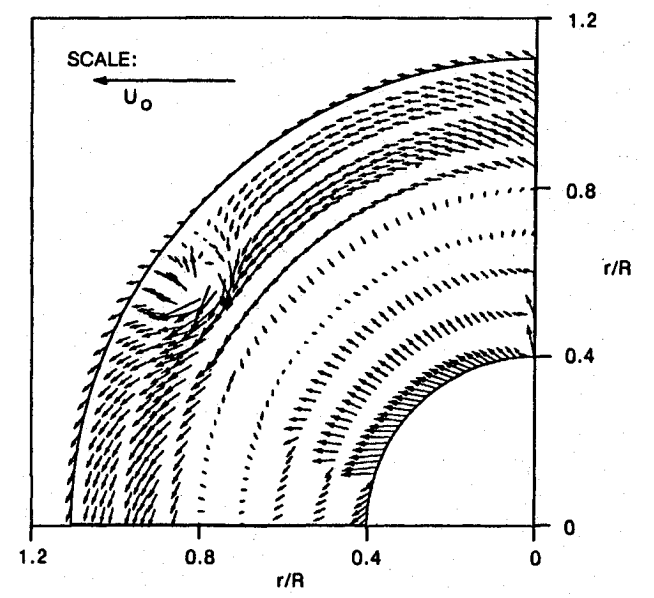

Fig. 5 Flowfield velocity vectors in propeller plane of rotation (every tenth data point shown).

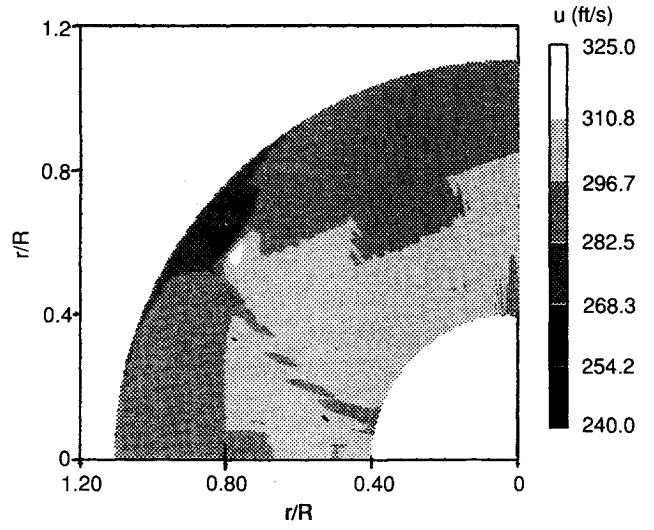

Fig. 6 Propeller flowfield axial velocity.

has been plotted in the azimuthal direction. Although this makes it impossible to view some features, such as the blade viscous wake, it serves to highlight the vortex region.

Another form of presenting the data is shown in Fig. 6, which is a contour plot of the axial velocity. Here, again, the vortex region is clearly defined by the adjacent high and low regions of velocity. When the data is viewed in this manner, one notices the tight, well-defined spatial features of the tip vortex/leading-edge vortex structure. It appears to be localized in the blade tip region, as one would expect for a propeller operating at cruise.[4] This figure also highlights the viscous wake, visible as a velocity defect along points defining the blade trailing edge.

Evidence of a vortex axial velocity, or core velocity, defect is obtained by performing a coordinate transformation on the data that effectively rotates the viewing plane about the radial coordinate axis by various amounts. This transformation is performed in the polar coordinate system at each tangential (i.e., azimuthal) location in space along the entire radial span. This viewing technique was used by Lavrich[10] in his recent analysis of another set of propfan wake data. The transformation, or viewing angle rotation, is somewhat difficult to visualize because the radial direction changes (relative to a fixed cartesian coordinate system) at each azimuthal location. This transformation is necessary in order to isolate the axial velocity from vortex swirl velocity effects. If the adjacent high and low velocity regions are purely the result of the vortex not being aligned with the x axis, as described earlier, then a coordinate transformation that places the axial direction more in line with the vortex core should smooth out this feature. The vortex swirl velocity would no longer add to the axial velocity on the inboard side of the vortex nor subtract from it on the outboard side.

A series of such transformations was performed over a range of rotation angles from 0 to 60 deg. This range extends well past the propeller swirl angle (ϕ = 48 deg). Although the transformations did have the effect of lowering the inboard high-velocity region, they did not remove the velocity defect on the outboard side. A sample of this effect is shown in Fig. 7, where the viewing angle is rotated from 5 to 15 deg in 5-deg increments. The 0-deg case is shown in Fig. 6. These figures show that the peak velocity on the inboard side of the vortex is progressively reduced with increasing rotation, but that an outboard velocity defect remains. There did not appear to be any transformation geometry or viewing angle that eliminated the low-velocity region. Thus, it is concluded that this region represents a local axial velocity defect and is not merely a result of the choice of coordinate system.

Wake Roll-Up

The perturbations to the tangential and radial velocity components in the blade tip region that were noted earlier may be related to the presence of wake roll-up. This phenomenon is essentially a skewing or wrapping around of the blade wake structure in the outboard region of the blade near the tip. It is caused by the finite radius vortex sheet acting on itself.

Hanson[11] modeled the roll-up effect, with results shown in Fig. 8, using the following simplistic procedure. A vortex sheet was represented by a line of discrete vortices with centers placed along the X axis (spanwise direction). The vortex sheet may be visualized as fixed to a blade trailing edge that would rotate in the negative Y direction. The strength of the vortices varied with X corresponding to an elliptic loading (or circulation) distribution along the span. At time t = 0, each vortex was permitted to induce motion on all of the others. With increasing time, the vortex sheet distorts, as shown by the plot on the right on the lower portion of Fig. 8. The increase in roll-up could represent either increased distance downstream or increased loading. For present purposes, it will be viewed as increased loading at a fixed instant of time and a fixed location near the blade trailing edge. The top portion of Fig. 8 shows the calculated radial and tangential velocity components plotted as a function of distance Y along the measurement line. A viscous wake is superimposed on the tangential velocity result since the simple calculation procedure cannot account for viscous effects.

Figure 8 shows sharp, predictable behavior for both velocity components for the case of insignificant roll-up on the left. On the right, where wake roll-up is pronounced, the effect

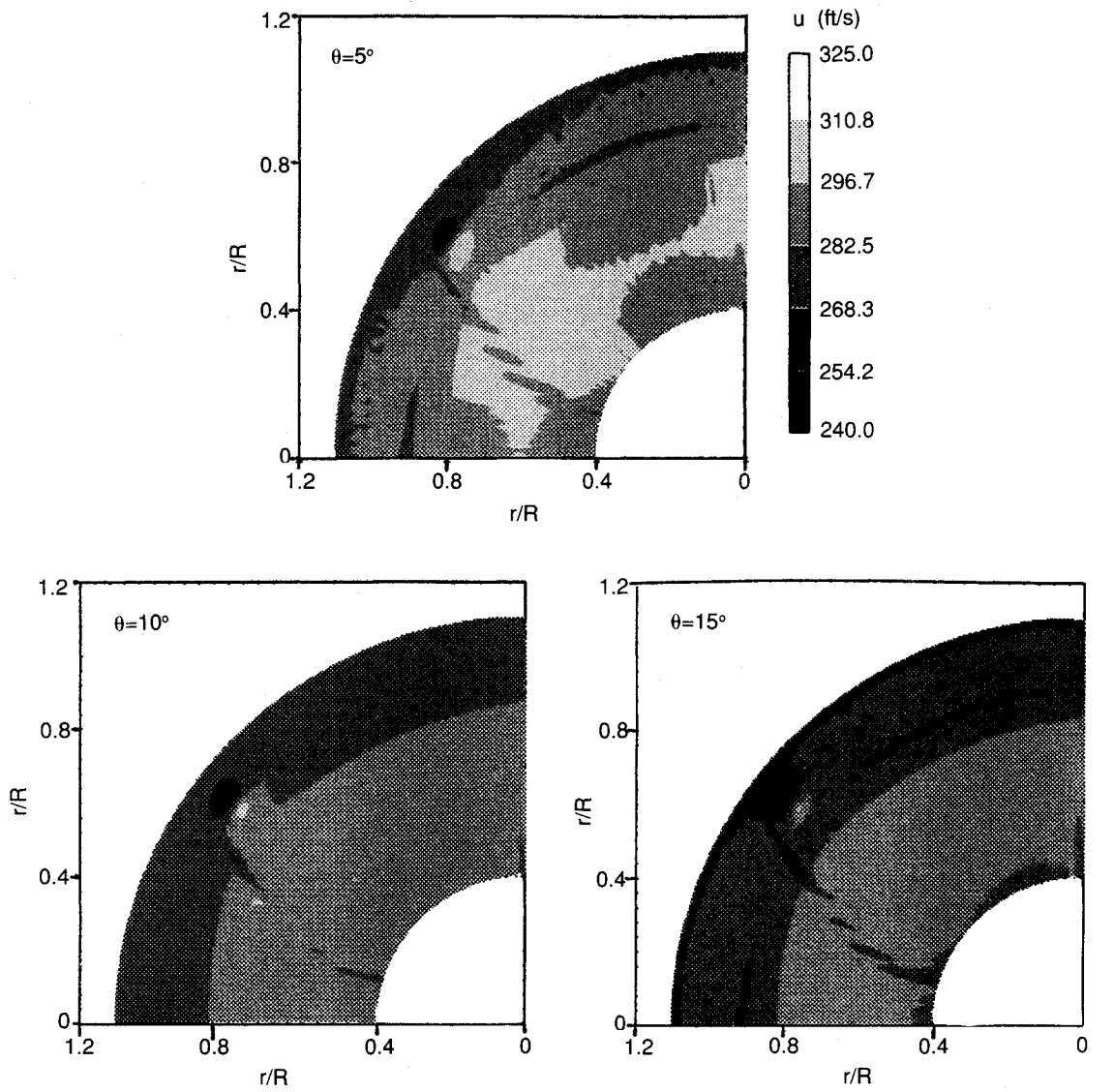

Fig. 7 Propeller flowfield transformed axial velocity.

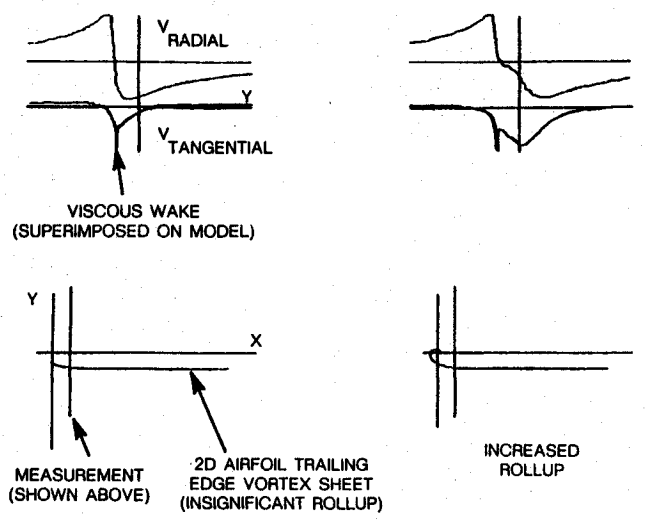

Fig. 8 Two-dimensional calculation of effect of roll-up on wake velocity components (From Hanson[11]).

on the velocity components is signified by a change in the basic features. Broadening of the wakes, along with profile perturbations quite similar to those observed in the data of Fig. 3, are seen. In particular, the velocity components at $r/R = 0.92$ are quite similar to those of the pronounced roll-up calculation case in terms of the profile shapes. Although the calculation procedure is simple and does not model all of the physics present in the propfan data (i.e., viscous effects), it does provide qualitative evidence that wake roll-up may be an important phenomenon to include in future propfan wake models.

Flow Visualization Results

As described earlier,[3,4] a fluorescent oil blade surface flow visualization technique was used to help characterize the blade tip vortex/leading-edge vortex structure. Data was obtained for the simulated cruise case as well as for a takeoff case for comparison purposes. These results are shown in the form of photographs of the blade suction surfaces in Fig. 9. The blade leading-edge vortex is indicated by a higher concentration of oil and tracer pigment in the outboard region and by a distinct change from the predominantly radial streak direction. Where the flow is attached to the blade and skin friction levels are high, much of the oil and tracer have been removed and the streaks possess a downstream directional component in addition to their radial component. The radial component is always present and is due to the centrifugal force imparted to the oil by the blade rotation. The leading-edge vortex reattachment line is indicated by the change in streak direction. Beneath the vortex, where skin friction levels are lower, the oil is flowing essentially radially outward.

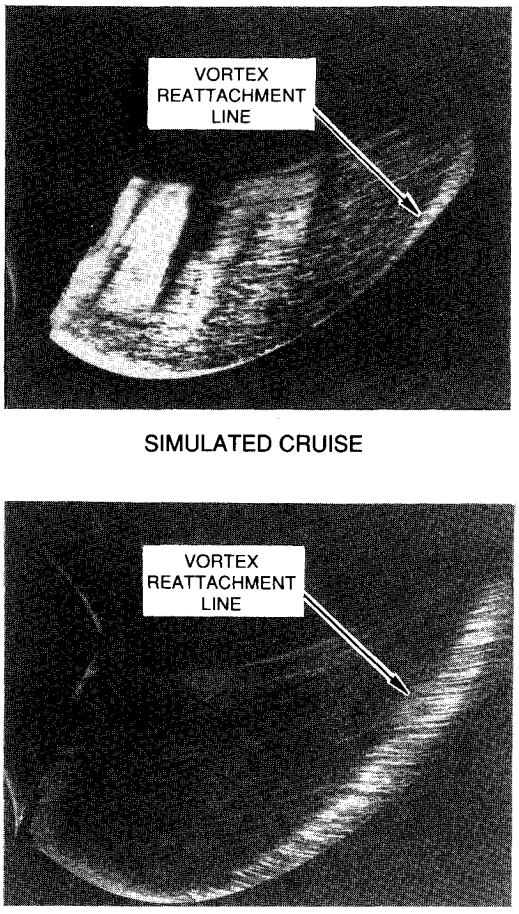

Fig. 9 Blade surface flow visualization showing leading-edge vortex (blade suction surface shown).

The vortex structure for the simulated cruise condition occupies only a small portion of the blade, and the formation process begins fairly far outboard near the tip region. This is in agreement with the hot wire results, which show a spatially small vortex near the tip. The takeoff case, however, possesses a much larger leading-edge vortex structure. The formation process begins significantly farther inboard and extends over a much larger portion of the blade. The flow visualization results imply that the downstream structure would in this case be spatially larger than that of the simulated cruise condition. The vortex core velocity defect may be spatially larger in this case as well, and could represent a significant takeoff noise source.

Concluding Remarks

The overall problem addressed in this article was the analysis of the aerodynamics downstream of a propfan. The present study involved blade-synchronized, three-dimensional periodic velocity measurements downstream of a single-rotation propfan (CRP-X1) operating at a simulated cruise condition.

As a result of this study, a set of three-dimensional velocity data defining the propfan downstream flowfield was obtained. A vortex core axial velocity defect was identified in the outboard portion of the tip region flowfield. This feature could be important in understanding the aerodynamic performance and noise associated with a downstream rotor in a counter-rotation propfan configuration, where wakes generated upstream impact the rotor. The tip vortex/leading-edge vortex structure appears to be spatially small and well defined at cruise, based on both the hot wire measurements and the flow visualization results. The vortex structure appears to be much larger for the takeoff case.

Local perturbations were identified in the tip region tangential and radial velocity components, which bear qualitative similarity to simple calculation predictions of wake roll-up features. If wake roll-up is an aerodynamic feature of propfan blades, existing performance and noise prediction methodologies may need to model this phenomenon. At this point, further experimental and analytical investigation of propfan flowfields is needed before a firm statement regarding the possible presence of wake roll-up, or its significance, may be made.

Acknowledgments

The work described in this article was supported by Hamilton Standard Division of United Technologies Corporation and by the United Technologies Research Center (UTRC) corporate-sponsored internal research program. The five-bladed propfan model was supplied by NASA Lewis Research Center and Hamilton Standard. Special thanks is due to Eric Johnson of Pratt and Whitney for his efforts relative to data reduction, Joel Wagner of UTRC for performing an uncertainty analysis of the hot wire data, and David Edwards of UTRC for preparing the three-dimensional visualization capability used in generating several key figures. Thanks is also due to Donald Hanson and Bernard Magliozzi of Hamilton Standard for their technical guidance throughout the course of this effort and to Robert Schlinker of UTRC for management of the program.

References

[1]Hanson, D. B., and Patrick, W. P., "Near Wakes of Advanced Turbopropellers," AIAA Paper 89-1095, April 1989.

[2]Podboy, G. G., and Krupar, M. J., "Laser Velocimeter Measurements of the Flowfield Generated by an Advanced Counterrotating Propeller," AIAA Paper 89-0434, Jan. 1989.

[3]Hanson, D. B., "Propeller Noise Caused by Blade Tip Radial Forces," AIAA Paper 86-1892, July 1986.

[4]Vaczy, C. M., and McCormick, D. C., "Study of Leading Edge Vortex and Tip Vortex on Prop-Fan Blades," ASME Report 87-GT-234, May 1987.

[5]Paterson, R. W., Vogt, P. G., and Foley, W. M., "Design and Development of the United Aircraft Research Laboratories Acoustic Research Tunnel," AIAA Paper 72-1005, Sept. 1972.

[6]Thermo Systems, Inc., "IFA 100 Intelligent Flow Analyzer Instruction Manual," Thermo Systems, Inc., St. Paul, Minnesota, 1983.

[7]Freymuth, P., "Frequency Response and Electronic Testing for Constant Temperature Hot-Wire Anemometers," *Journal of Physics E: Scientific Instruments*, Vol. 10, July 1977, pp. 705–710.

[8]Tillman, T. G., Simonich, J. C., and Wagner, J. H., "Hot Wire Measurements Downstream of a Prop-Fan," AIAA Paper 89-2698, July 1989.

[9]Edwards, D. E., "Three-Dimensional Visualization of Fluid Dynamic Problems," AIAA Paper 89-0136, Jan. 1989.

[10]Lavrich, P. L., private communication, June 1989.

[11]Hanson, D. B., private communications, 1987.